Monte Carlo Calculation of Second Virial Coefficients for Linear and Star Chains in a Good Solvent

Ana M. Rubio and Juan J. Freire*

Departamento de Química Física, Facultad de Ciencias Químicas, Universidad Complutense, 28040 Madrid, Spain

Received March 4, 1996; Revised Manuscript Received June 28, 1996[⊗]

ABSTRACT: Second virial coefficients and radii of gyration for an off-lattice model of linear and star polymer chains in a good solvent (or excluded volume conditions) have been obtained by means of a Monte Carlo method. The results are discussed in terms of the dimensionless interpenetration factor, which combines these two quantities. Comparisons with theoretical prediction from the renormalization group theory and with existing simulation and experimental data are performed for the different types of chains.

Introduction

The osmotic second virial coefficient, A_2, of a polymer solution is an interesting property that has been the object of numerous theoretical and experimental studies.[1,2] This property becomes equivalent to the second virial coefficient[3] if the site interactions are described by a solvent-mediated potential of the mean force. Usually, data are presented in terms of an adimensional quantity, the interpenetration factor, depending also on the molecular weight, M, and the mean quadratic radius of gyration, $\langle S^2 \rangle$,

$$\psi^* = 2A_2M^2/N_A(4\pi\langle S^2\rangle)^{3/2} \quad (1)$$

where N_A is Avogadro's number.

For the fully developed excluded volume regime (long chains in a good solvent), renormalization group calculations have predicted that this factor (obtained by considering the intermolecular interaction between a pair of flexible chains) is a universal constant. For linear chains in three dimensions, it has the value[3−7]

$$\psi^* = 0.25-0.27 \quad (2)$$

Similar calculations have also been performed for different branched structures as regular star chains in the same good solvent conditions.[6−8] On the other hand, there are abundant bibliographic experimental data of A_2 and ψ^* for linear[2,8,9] and star chains in good solvents.[8,10−12] (A summary of theoretical and experimental results can be found in Table 1). The agreement between theoretical and experimental interpenetration factors is reasonably good for linear chains, but it becomes worse with a significant degree of branching. Indeed, renormalization group theory calculations for a regular star with a large number of arms ($F = 18$) indicate an unphysical negative value[8] for ψ^* because of the ill-behaved nature of the perturbation expansion for large F. The theory is then limited to "light branching" where the parameter characterizing the degree of branching remains small. It should also be considered that the experimental data are considerably scattered in some of these cases, which somehow complicates the comparison with theory. Given this situation, the necessity of performing numerical simulations for this property with adequate polymer models can be easily understood.

[⊗] Abstract published in *Advance ACS Abstracts,* September 1, 1996.

Table 1. Summary of Previous Results for g and ψ^*

	g_S	ψ^*	A_2^{star}/A_2^{linear}
Linear Chains			
$F = 2$			
exp[a]		0.24−0.27	
RG[b]		0.249; 0.269	
lattice MC[c]		0.247	
Stars			
$F = 4$			
exp[d]	0.58−0.63	0.46−0.55	0.89−0.96
exp[e]	0.61	0.43−0.45	0.89
RG[f]	0.631	0.517	0.923
lattice MC	0.61[g]	0.43[h]	
$F = 6$			
exp[d]	0.42−0.48	0.65−0.67	0.84−0.88
RG[f]	0.453	0.793	0.81
lattice MC	0.431[g]	0.63[h]	
earlier work[i]	0.44		
$F = 12$			
exp[d]	0.24	1.10	0.51
RG[f]	0.248	1.35	0.36
lattice MG[g]	0.234		
earlier work[i]	0.23		
$F = 18$			
exp[d]	0.17−0.21	1.10−1.35	0.32−0.41
RG[f]	0.173		
earlier work[i]	0.17		

[a] Experimental data from refs 2, 8, and 9. The range of experimental data is a realistic estimation from different data (some reported data can be outside this range). A more detailed description of samples and data can be found in ref 8. [b] Renormalization group theory[3−5] (differences between the two values are explained in the text). [c] Monte Carlo simulation for long chains in a cubic lattice.[5] [d] Experimental data from refs 8 and 10−12. See footnote *a* for the validity of ranges and further information. [e] Data from experimental work in progress.[25] [f] Renormalization group theory.[6,7] [g] Monte Carlo simulation for long chains in a tetrahedral lattice.[26] [h] Recent Monte Carlo simulations for $N/F = 10-80$ in a cubic lattice (mean values).[28] [i] Extrapolations from previous simulations with the same model (short chains).[23]

For linear chains, very accurate simulation studies have been carried out recently[5,13] through the basic model of self-avoiding (or athermal) linear chains in a cubic lattice.[14] A similar model, but with an attractive term between neighbor units, has also been used to characterize the Θ point[15,16] (i.e. the temperature for which $A_2 = 0$). The latter type of study has also been carried out for star chains[17] up to $F = 6$. Recently, the freely jointed linear chain with athermal units[18] or with units interacting through the Lennard-Jones potential[19] has also been investigated, though these results for A_2 have not been interpreted in terms of the interpenetration function.

S0024-9297(96)00346-4 CCC: $12.00

In the present work, we also use an off-lattice model,[20] consisting of Gaussian units of length unit b, with a Lennard-Jones potential that describes interactions between non-neighboring units. We compute A_2 by evaluating the averaged Mayer function of Monte Carlo generated pairs of chains, a method that we previously employed for calculating binary interactions of *n*-alkanes in the gas phase, represented by the rotational isomeric model.[21] According to the reasons given in previous paragraphs, our main aim is to obtain the interpenetration factor for linear and uniform star chains in good solvent (or excluded volume) conditions and discuss the results in terms of the existing theoretical predictions and experimental data.

Model and Methods

The off-lattice model consists of N Gaussian units of length b, i.e. N units separated from their neighbors through bonds whose lengths are not constant but follow a Gaussian distribution with root-mean-square length b, in the absence of intramolecular interactions. (b is considered the length unit in our calculations.) Non-neighboring units interact, however, through a Lennard-Jones potential, with the size parameter kept constant, $\sigma = 0.8b$. This model has previously been employed to reproduce other conformational properties of linear and star chains,[22,23] characterizing the Θ state and the transition from the collapsed state to the excluded volume regime[24] in terms of the reduced energy in the well depth of the potential ϵ/k_BT. (k_BT is the Boltzmann factor.) In accordance with this characterization, the value $\epsilon/k_BT = 0.1$ reproduces the excluded volume or good solvent conditions, giving a value of ν defined

$$\langle S^2\rangle^{1/2} \approx N^{\nu} \tag{3}$$

very close to the best current estimate of this theoretical value of this critical exponent,[5] $\nu = 0.588$. This agreement is obtained even for remarkably short chains.[20] Consequently, we adopt $\epsilon/k_BT = 0.1$ also for the present study of second virial coefficients. The value of this somewhat arbitrary choice of the interaction energy is that long-range dimensionless quantities approach their excluded volume asymptotic limit more rapidly than they would otherwise.

Our method is based in considering pairs of independent conformations generated in two different and parallel stochastic Monte Carlo processes. The details of the Monte Carlo algorithm have previously been described.[22] We generate a first chain in the process with moderate energy, avoiding overlapping between units. Then we generate other conformations of the same sample by selecting a bond vector in the preceding chain and resampling its components from the Gaussian distribution with zero mean and square deviation equal to 1/3. The rest of the chain up to its closest end (or the arm end in the star) is rotated by means of three randomly selected Euler angles and then connected to the new vector. This way, the method can be considered as a particular version of the Pivot algorithm, which has been proved to be very efficient for self-avoiding lattice chains.[5]

Calculation of the second virial coefficient was performed through a method basically inspired by the procedure described in ref 21. For each pair of Monte Carlo generated chain conformations, we choose a distance r between centers of masses and put the center of molecule 2 on a random point of the sphere (centered in the center of masses of chain 1) with radius r and a choice of polar coordinates in terms of two random values for $\cos\theta$ and Φ. Then the intermolecular interactions between the two chains are obtained as

$$U_{\text{inter}}(r,\theta,\Phi) = \sum_{i,\text{chain 1}}^{N} \sum_{j,\text{chain 2}}^{N} U_{\text{LJ}}(R_{ij}) \tag{4}$$

where the summation terms correspond to values of the Lennard-Jones potential for intermolecular interactions between units i and j. We have performed several calculations of U_{inter} with different random angles in order to fully explore the different orientations for every particular pair of conformations. In the present case of excluded volume conditions, however, a single orientation for a pair of conformations is revealed to be adequate. Then we change r and obtain again one or several values of U_{inter} in a similar way (same pair of conformations and same orientations). From these results, we evaluate the averaged Mayer function for each of the different values of r,

$$f_M(r) = \langle \exp(-U_{\text{inter}}/k_BT)\rangle - 1 \tag{5}$$

obtaining arithmetic means over all the sampled pairs of differently oriented conformations. Alternatively, we can perform the evaluation of U_{inter} only for a fraction of the generated pairs of conformations. However, we have verified that the best accuracy for excluded volume conditions is obtained when the intermolecular energy is calculated for all the pairs of conformations contained in the two parallel samples. Finally, we obtain

$$\Gamma_2^* \equiv A_2M^2/N_A = -2\pi \int_{r=0}^{\infty} f_M(r) r^2\, dr \tag{6}$$

Numerical integrations are practically truncated at a value of $r_{\max}$ that is verified to be adequate for each chain length. It varies from $30b$ (short chains) to $90b$ (longest chains). Integrations are evaluated by dividing the range of r values in about 30 intervals, whose widths are not constant but are smaller in the region around the maximum of the function $r^2 f_M$. We have performed 4 or 8 completely independent evaluations of Γ_2^* (with different seed numbers that determine the initial conformations of the parallel samples). In each of these runs, we have attempted 30 000 Pivot moves for equilibrium and 50 000 further moves for the calculation of properties. Averaged values of the radius of gyration are obtained as arithmetic means over the different samples in a similar way. Some of these values for $\langle S^2\rangle$ were calculated with the same model and reported in previous work.[20,22−24]

Results and Discussion

Table 2 contains our numerical values of Γ_2^* and $\langle S^2\rangle$, obtained for different chain lengths and architectures (linear or regular star chains of various values of F). Figure 1 shows the N dependence for the dimensionless ratio of dimensions of a given star chain to that of a linear chain with the same number of units

$$g_S = \langle S^2\rangle_{\text{linear}}/\langle S^2\rangle_{\text{star}} \tag{7}$$

According to this figure, linear fits of g_S vs $1/N$ have been used to obtain extrapolated values of g_S in the long-

Table 2. Numerical Results Obtained from the Simulations

F	N	$\langle S^2 \rangle$	Γ_2^*	ψ^*	g_s
2	2	0.2503 ± 0.0004	1.484 ± 0.002	0.532 ± 0.003	
	3	0.4862 ± 0.001	2.808 ± 0.002	0.372 ± 0.002	
	4	0.7189 ± 0.002	4.433 ± 0.008	0.326 ± 0.002	
	5	0.966 ± 0.002	6.375 ± 0.002	0.301 ± 0.002	
	7	1.478 ± 0.003	11.26 ± 0.03	0.281 ± 0.002	
	9	2.010 ± 0.005	17.17 ± 0.05	0.270 ± 0.003	
	13	3.15 ± 0.02	32.6 ± 0.2	0.262 ± 0.006	
	17	4.33 ± 0.02	51.6 ± 0.3	0.257 ± 0.005	
	19	4.96 ± 0.03	62.5 ± 0.2	0.254 ± 0.004	
	21	5.61 ± 0.02	74.7 ± 0.2	0.252 ± 0.003	
	25	6.88 ± 0.02	100.7 ± 0.3	0.250 ± 0.002	
	29	8.25 ± 0.04	131.9 ± 0.4	0.250 ± 0.003	
	37	11.0 ± 0.2	199.8 ± 0.5	0.246 ± 0.008	
	49	15.40 ± 0.06	331 ± 2	0.246 ± 0.003	
	61	19.9 ± 0.1	483 ± 2	0.244 ± 0.004	
	73	24.6 ± 0.1	662 ± 10	0.244 ± 0.009	
	85	29.40 ± 0.05	859 ± 4	0.242 ± 0.001	
	109	39.30 ± 0.07	1327 ± 9	0.242 ± 0.002	
	145	55.5 ± 0.2	2233 ± 6	0.242 ± 0.002	
	217	89.35 ± 0.05	4527 ± 22	0.241 ± 0.006	
	289	125 ± 1	7433 ± 42	0.239 ± 0.004	
4	5	0.788 ± 0.001	6.37 ± 0.02	0.417 ± 0.003	0.805 ± 0.003
	9	1.43 ± 0.003	16.258 ± 0.004	0.43 ± 0.01	0.716 ± 0.003
	13	2.144 ± 0.004	29.98 ± 0.07	0.429 ± 0.003	0.681 ± 0.006
	17	2.87 ± 0.01	46.9 ± 0.2	0.433 ± 0.006	0.663 ± 0.005
	21	3.66 ± 0.01	67.6 ± 0.2	0.43 ± 0.01	0.652 ± 0.004
	25	4.48 ± 0.01	91.1 ± 0.1	0.431 ± 0.002	0.651 ± 0.003
	37	6.95 ± 0.03	178.4 ± 0.2	0.437 ± 0.004	0.63 ± 0.01
	49	9.63 ± 0.06	293 ± 1	0.440 ± 0.007	0.625 ± 0.006
	61	12.39 ± 0.06	427 ± 2	0.440 ± 0.007	0.623 ± 0.006
	73	15.2 ± 0.1	585 ± 3	0.443 ± 0.009	0.618 ± 0.006
	85	18.2 ± 0.1	760 ± 4	0.439 ± 0.008	0.619 ± 0.004
	109	24.5 ± 0.1	1176 ± 4	0.435 ± 0.006	0.623 ± 0.004
	145	34.4 ± 0.3	1953 ± 9	0.43 ± 0.01	0.620 ± 0.008
	217	54.0 ± 0.3	3953 ± 20	0.447 ± 0.008	0.604 ± 0.004
	289	76.3 ± 0.8	6576 ± 31	0.44 ± 0.01	0.61 ± 0.01
6	37	5.20 ± 0.03	155.0 ± 0.9	0.59 ± 0.01	0.47 ± 0.01
	49	7.15 ± 0.02	251.2 ± 0.9	0.590 ± 0.007	0.464 ± 0.003
	73	11.19 ± 0.06	502 ± 3	0.60 ± 0.01	0.455 ± 0.004
	85	13.42 ± 0.07	654 ± 2	0.597 ± 0.008	0.458 ± 0.003
	109	17.58 ± 0.05	1016 ± 2	0.619 ± 0.005	0.447 ± 0.002
	145	24.4 ± 0.1	1654 ± 8	0.62 ± 0.01	0.440 ± 0.003
	217	39.2 ± 0.3	3394 ± 32	0.62 ± 0.02	0.439 ± 0.004
	289	54.6 ± 0.5	5588 ± 39	0.62 ± 0.02	0.437 ± 0.007
12	37	3.31 ± 0.01	111.7 ± 0.7	0.83 ± 0.01	0.300 ± 0.006
	49	4.36 ± 0.03	178.6 ± 0.6	0.88 ± 0.01	0.283 ± 0.003
	73	6.67 ± 0.04	348 ± 2	0.91 ± 0.02	0.271 ± 0.002
	85	7.83 ± 0.05	453 ± 2	0.93 ± 0.02	0.266 ± 0.002
	109	10.1 ± 0.01	687 ± 7	0.96 ± 0.02	0.260 ± 0.003
	145	13.6 ± 0.06	1111 ± 7	0.995 ± 0.008	0.24 ± 0.01
	217	21.6 ± 0.02	2268 ± 8	1.014 ± 0.008	0.242 ± 0.002
	289	29.8 ± 0.02	3643 ± 30	1.01 ± 0.02	0.238 ± 0.003
18	37	2.66 ± 0.02	91 ± 1	0.94 ± 0.03	0.242 ± 0.006
	73	5.09 ± 0.04	268 ± 3	1.05 ± 0.04	0.207 ± 0.002
	109	7.68 ± 0.07	538 ± 5	1.14 ± 0.04	0.195 ± 0.002
	145	10.29 ± 0.04	857 ± 7	1.17 ± 0.03	0.185 ± 0.001
	217	15.6 ± 0.1	1722 ± 37	1.25 ± 0.07	0.174 ± 0.001
	289	21.2 ± 0.2	2654 ± 19	1.22 ± 0.03	0.170 ± 0.003

chain limit. Figure 2 shows the N dependence of the results obtained for the interpenetration factor, according to eq 1. The values of ψ^* and g_S are also contained in Table 2, together with their estimated error bars. It is apparent that the ψ^* values reach a constant asymptotic long-chain limit for small or moderate values of N. Therefore, numerical fits similar to those employed for the numerical treatment of g_S or fits considering a theoretical finite size correction term[5] of the type $N^{-\Delta_1}$, with $\Delta_1 < 1$, are clearly not useful for these data. It seems reasonable to assume that star chains with a high number of arms reach the limit more slowly than lightly branched chains because of the more important central core effects. Consequently, we have decided to obtain a final estimation of the long-chain limit of ψ^* for each chain type by evaluating an arithmetic mean of all the numerical values corresponding to an F-dependent range of chain lengths. This range is defined to contain chains long enough so that error intervals associated with their values of ψ^* clearly overlap. Our long chain limit estimations for both g_S and ψ^* are contained in Table 3, together with the fitting exponents ν and γ, obtained over the same range of values of N employed in the determination of ψ^*. The latter exponent is defined as

$$\Gamma_2^* \cong N^{\gamma} \tag{8}$$

and, consistent with the assumption of a universal

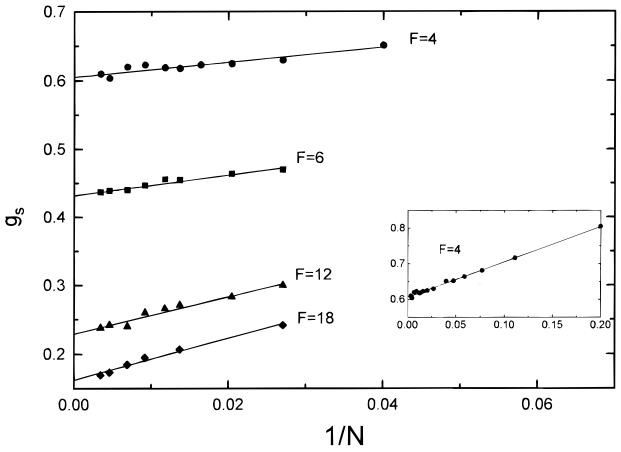

Figure 1. g_S vs $1/N$ for different star chains. Symbols from top to bottom: $F = 4$, circles; $F = 6$, squares; $F = 12$, triangles up; $F = 18$, diamonds. Inset: full range of chain lengths for $F = 4$.

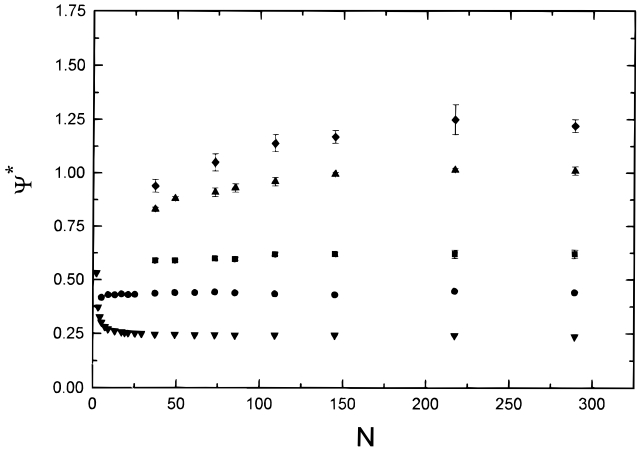

Figure 2. ψ^* (with error bars when significant) vs N for linear ($F = 2$) and star chains. Symbols from bottom to top: Linear, triangles down; $F = 4$, circles; $F = 6$, squares; $F = 12$, triangles up; $F = 18$, diamonds.

constant for ψ^*, should be related to ν through the relationship

$$\gamma = 3\nu \tag{9}$$

As expected, the exponent ν for linear chains is very close to the best theoretical prediction quoted in the preceding section. However, the values of ν are smaller for stars, and the decrease is more significant for increasing number of arms. Moreover, ν changes significantly with the range of chain lengths used for its determination. This effect is clearly caused by finite size effects, which are more important as the number of arms increases, since the stars have a larger central core and the averaged chain size is smaller. This effect is important in the present model and also in experimental samples. Thus, though experimental values of ν consistent with the theory are obtained for lightly branched stars of moderately high molecular weights, the experimental radii of gyration[8] for $F = 18$ yield values of $\nu \cong 1.10$ clearly far away from the critical value.

Our fitted result for γ for linear chains agrees satisfactorily with the theoretical value expected from eq 9. A good agreement is also found for lightly branched stars, especially when the fitted value of ν, instead of its theoretical value, is introduced in eq 9. Moreover, the relationship between fitted exponents is also approximately maintained in the case of highly armed stars, reflecting an early approach of ψ^* to its asymptotic value in all cases. This early approach is especially noticeable in the case of linear chains, since previous simulation values with the lattice model only approach the limiting value for much longer chains. Thus, results[13] obtained from direct enumeration give $\psi^* = 0.658$ for $N = 2$ and $\psi^* = 0.388$ for $N = 7$. Moreover, in Table 6 of ref 5 we can observe that $\psi^* = 0.277$ for $N = 100$ and $\psi^* = 0.263$ for $N = 300$ and that this magnitude still shows a slow but monotonous decrease for very long chains, $\psi^* = 0.256$ for $N = 1000$ and $\psi^* = 0.248$ for $N = 80\,000$. Even though the off-lattice model prevents us from using special techniques to get the extremely good accuracy of the lattice values (or reaching very high chain lengths), it is satisfactory that, as shown in Table 2, our final estimation for the asymptotic limit, $\psi^* = 0.242$, is within the error bars (± 0.004 on average) of our numerical results for ψ^* for all values of $N \geq 61$. However, we should also point out that our final estimation of this limit is slightly smaller than the limit obtained in ref 5 for chains in a cubic lattice $\psi^* = 0.247$. (We obtain results similar to or smaller than this latter limit for all our chains with $N \geq 29$.)

Another interesting feature of the variation of ψ^* with N is whether the asymptotic limit for long chains is reached from above or from below. The two-parameter renormalization theory through second order in ϵ-perturbation theory predicts an approach from below.[6] However, the lattice simulations show the opposite behavior.[5,13] Experimental data for short and longer polymer chains in good solvents[2,9] are qualitatively consistent with the latter behavior, and the discrepancy with theory has been attributed to stiffness. However, it has been recently argued[5,13] that two-parameter theory cannot give correctly universal coefficients to describe the N-dependent deviation from asymptotic behavior. This point could be checked in a nonperturbative calculation based on the Domb−Joyce model,[2,13] the discrete analog of the two-parameter model. As it is heuristically discussed in ref 5, very short chains practically behave as hard spheres for which the value of ψ^* is much higher than the asymptotic limit for linear chains. By this reasoning, there is no need for considering stiffness to explain the approach from above. Since our chains are flexible even when they are very short ($N = 2$ corresponds to a Gaussian segment with two interacting units at the ends), they are adequate to check this point. Our Monte Carlo values for ψ^* for very short chains ($N = 2-17$) are clearly greater than the asymptotic limit. Since stiffness is, anyway, crucial in determining whether the limit is reached in a slow or fast way, we conclude that the slow approach to the asymptotic limit in the lattice model should be associated with its higher rigidity.

Our asymptotic values of ψ^* for linear chains contained in Table 3 can be compared with those obtained from renormalization group theory and from experiments, summarized in Table 1. As we discussed before, our value for linear chains is close to the value obtained with simulations of extremely long chains in a lattice. The latter result is about 0.02 smaller than the theoretical prediction of renormalization group theory (expansion in powers of $\epsilon = 4 - d$ up to second order[3,4]). However, if the expansion coefficients are modified[4] to enforce the known exact values for $d = 1$, $\psi^* = 0.249$, is obtained,[5] a value practically identical to the asymptotic limit of the lattice simulations and, therefore, also

Table 3. Long Chain Limit Estimations and Fitting Exponents

F	N	g_S[a]	ψ^*[b]	$(A_2^F/A_2^{F=2})$[c,d]	ν[e]	$(\gamma/3)$[e]
2	37−289		0.2422 ± 0.0004		0.592 ± 0.001	0.588 ± 0.001
4	37−289	0.607 ± 0.002	0.439 ± 0.002	0.883 ± 0.002 0.86 ± 0.01	0.583 ± 0.002	0.584 ± 0.001
6	109−289	0.432 ± 0.003	0.6193 ± 0.0003	0.752 ± 0.005 0.73 ± 0.01	0.581 ± 0.013	0.582 ± 0.002
12	145−289	0.231 ± 0.002	1.005 ± 0.006	0.496 ± 0.003 0.47 ± 0.01	0.567 ± 0.007	0.579 ± 0.003
18	145−289	0.160 ± 0.001	1.21 ± 0.04	0.374 ± 0.008 0.33 ± 0.02	0.518 ± 0.005	0.547 ± 0.007

[a] Extrapolations from g_S vs $1/N$ fittings. [b] Arithmetic means over the indicated chain length ranges. [c] First set of values (above): arithmetic means over the indicated chain length ranges. [d] Second set of values (below): from asymptotic values of g_S and ψ^* (eq 10). [e] From log−log fittings to the theoretical scaling laws in the indicated chain length ranges.

in close agreement with all the present results for moderately long chains. It should be pointed out, however, that the latter modification worsens the agreement with simulation results for other quantities as the ratio of the quadratic average end-to-end distance to $\langle S^2 \rangle$ (see Appendix D in ref 5 for further details). Experimental data for linear chains[2,8,9] are generally consistent with these conclusions, though their higher errors preclude them from being adequate for a precise elucidation of the remaining theoretical discrepancies.

The simulation results for stars can also be compared with theoretical and experimental data. Simulation values of the ratio g_S for excluded volume conditions with the same model were reported some time ago,[23] and a revision including longer chains performed for 12-arm stars[22] confirmed the previous estimation for this particular case. The present results cover the case $F = 4$ (not considered in our previous investigations) and are extended to longer chains for all the values of F. It is found now that our earlier values for the asymptotic limit, estimated through extrapolations from their dependence with $1/N$, were surprisingly good even for the $F = 18$ chain (for which we only considered previously 3 or fewer units per arm!). Moreover, the agreement of all these results, including now the $F = 4$ case, with experimental data[8,25] is excellent. Renormalization group theory predictions[6−8] for g_S in the long-chain limit are also in very good agreement with the experimental data and our simulation results for the considered range of values of F. It should also be mentioned that these ratios are in good agreement with much simpler calculations performed by assuming that both stars and linear chains obey Gaussian statistics,[8] as non-Gaussian effects in the numerator and denominator nearly cancel out. Simulations for very long star chains in a tetrahedral lattice[26] have also confirmed this point, and they are in excellent agreement with our present off-lattice results.

According to the results shown in Figure 2 and Table 2, already mentioned, our values of ψ^* reach a constant asymptotic value for moderately short chains and for slightly or moderately branched stars, $N = 49$ for $F = 4$ and $N = 109$ for $F = 6$. For $F = 12$, we obtain a constant value for the three longest computed chains, $N = 145-289$, and something similar is found for $F = 18$, though the error bars are higher for this heavily armed star chain. It can be observed that these asymptotic limits for stars are always obtained from below, with increasingly more important and more persistent finite size effects, due to the building of a central core, for increasing values of F. However, our previous discussion of a higher hard-sphere limit for very short chains should also be borne in mind, since this limit, $\psi^* = 1.62$, is still considerably higher than our asymptotic result for $F = 18$, $\psi^* \cong 1.22$. Therefore, a competition between stiffness and central core effects can be expected for more rigid star chains. The smallest star chain considered in this work, $N = 5$, $F = 4$, still shows a slightly smaller value of ψ^* than longer chains of the same type. (Thus we have omitted the calculation of very short chains for other stars.)

Experimental data of ψ^* for stars[8,10−12] are in general agreement with our asymptotic data. A good summary of these data is given in ref 8. For $F = 4$ and 6, the existing values are somewhat scattered, and some of these values are smaller or higher than our limits with differences that do not exceed 0.1. However, our results for $F = 4$ are in excellent agreement with the most recent experimental data.[25] For $F = 12$, only one sample has apparently been investigated,[8,11,12] and the estimated value of ψ^* is higher than our limit. The data for $F = 18$ are more interesting since only one sample yields a value of ψ^* higher than our asymptotic limit, while the rest are close to it. The influence of N should be greater for this many-arm star with a large central core. In fact, the experimental data for the lowest molecular weights of a given polymer/solvent system (polybutadiene samples in cyclohexane[8,12]) are somehow similar to the smaller simulation values shown in Table 2 for the shorter chains. Therefore, the latter experimental data seem to support the approach to the asymptotic limit from below in the case of highly branched stars, as a consequence of core effects.

Renormalization group predictions for ψ^* reach up to the $F = 12$ case. (As mentioned in the Introduction, a physically incorrect negative value is predicted for $F = 18$ on account of the ill-behaved nature of the perturbation treatment for large F.) These theoretical values are always higher than our simulation values (and generally higher than the experimental data). The difference is already noticeable for $F = 4$; it reaches 0.17 for $F = 6$ and goes up to 0.34, i.e. 25%, for $F = 12$. Therefore, the performance of renormalization group calculations is poorer than in the case of the ratio g_S. It can be pointed out that renormalization group approaches exhibit also a deficient performance versus simulation for highly branched chains in some other applications. This is the case of the predictions for segregation between blocks in miktoarm polymers, performed in first order of ϵ, which turn out to be correct only for lightly branched chains.[27] A better theoretical approach would probably be established by developing a perturbative scheme for the large-F limit based on an expansion about the spherical model, similar to that employed in the theory of critical phenomena.

We have also considered the ratios of second virial coefficients of stars to those of homologous linear chains.

Experimental data for these ratios are contained in Table 1, together with renormalization group predictions. These predictions are obtained from those corresponding to g_S and ψ^* since, according to eqs 1 and 7, the ratios can be expressed as

$$\frac{A_2^{\text{star}}}{A_2^{\text{linear}}} = g_S^{3/2}\frac{\psi^*_{\text{star}}}{\psi^*_{\text{linear}}} \tag{10}$$

We have also calculated these ratios from the asymptotic limits for g_S and ψ^* and, in a more precise way, as arithmetic means over the ratios obtained directly from our simulation values of A_2 (these averages extend again over the mentioned ranges of N corresponding to practically constant values of ψ^* for the stars and linear chains). These two types of results are included in Table 3, where we observe a good agreement between them. Our asymptotic ratios are smaller than the renormalization group theory prediction for $F = 4$ and 6, but they are significantly larger than the theoretical value for $F = 12$. Moreover, our results agree with the most recent experimental data[25] for $F = 4$, although they are slightly smaller than most of the older data for $F = 4$ and 6. Finally, they also agree with the experimental data for the highly armed stars ($F = 12$, 18), taking into account the associated error bars.

After the present work was submitted for publication, new Monte Carlo data for the second virial coefficient of lightly branched star chains in a cubic lattice were reported.[28] These data correspond to the range $N/F = 10-80$ with $F = 3-6$. Although larger fluctuations in the values of ψ^* are observed, these new data are in good agreement with our results.

Acknowledgment. This work was supported by Grant No. PB92-0227 from the DGICYT, Spain.

References and Notes

(1) Yamakawa, H. *Modern Theory of Polymer Solutions*; Harper and Row: New York, 1971.
(2) Fujita, H. *Polymer Solutions*; Elsevier: Amsterdam, 1990.
(3) des Cloizeaux, J.; Jannink, G. *Polymers in Solution. Their Modelling and Structure*; Clarendon: Oxford, 1990.
(4) des Cloizeaux, J. *J. Physique* **1981**, *42*, 635.
(5) Li, B.; Madras, N.; Sokal, A. *J. Stat. Phys.* **1995**, *80*, 661.
(6) Douglas, J. F.; Freed, K. F. *Macromolecules* **1984**, *17*, 2344.
(7) Freed, K. F. *Renormalization Group Theory of Macromolecules*; Wiley: New York, 1987.
(8) Douglas, J. F.; Roovers, J.; Freed, K. F. *Macromolecules* **1990**, *23*, 4168.
(9) Huber, K.; Stockmayer, W. H. *Macromolecules* **1987**, *20*, 1400.
(10) Roovers, J.; Hadjichristidis, N.; Fetters, L. J. *Macromolecules* **1983**, *16*, 214.
(11) Huber, K.; Burchard, W.; Fetters, L. J. *Macromolecules* **1984**, *17*, 541.
(12) Toporowski, P. M.; Roovers, J. *J. Polym. Sci., Polym. Chem. Ed.* **1986**, *24*, 3009.
(13) Nickel, B. G. *Macromolecules* **1991**, *24*, 1358.
(14) Janssens, M.; Bellemans, A. *Macromolecules* **1976**, *9*, 303.
(15) Olaj, O. F.; Lantschbauer, W. *Ber. Bunsenges. Phys. Chem.* **1977**, *81*, 985.
(16) Bruns, W. *Macromolecules* **1984**, *17*, 2826.
(17) Bruns, W.; Carl, W. *Macromolecules* **1991**, *24*, 209.
(18) Yethiraj, A.; Honnell, K. G.; Hall, C. K. *Macromolecules* **1992**, *25*, 3979.
(19) Harismiadis, V. A.; Szleifer, I. *Mol. Phys.* **1994**, *81*, 851.
(20) Freire, J. J.; Pla, J.; Rey, A.; Prats, R. *Macromolecules* **1986**, *19*, 459.
(21) López Rodríguez, A.; Freire, J. J. *Mol. Phys.* **1988**, *63*, 591.
(22) Freire, J. J.; Rey, A.; Bishop, M.; Clarke, J. H. R. *Macromolecules* **1991**, *24*, 6494.
(23) Rey, A.; Freire, J. J.; García de la Torre, J. *Macromolecules* **1987**, *20*, 342.
(24) Rubio, M.; Freire, J. J.; Clarke, J. H. R.; Yong, C. W.; Bishop, M. *Macromolecules* **1995**, *102*, 2277.
(25) Okumoto, M.; Terao, K.; Nakamura, Y.; Teramoto, A. Private communication of a manuscript in preparation.
(26) Zifferer, G. *Makromol. Chem.* **1991**, *192*, 1555.
(27) Vlahos, C.; Horta, A.; Hadjichristidis, N.; Freire, J. J. *Macromolecules* **1995**, *28*, 1500.
(28) Ohno, K.; Shida, K.; Kimura, M.; Kawazoe, Y. *Macromolecules* **1996**, *29*, 2269.

MA960346N